# 3D-QSAR and Receptor Modeling of Tyrosine Kinase Inhibitors with Flexible Atom Receptor Model (FLARM)

Tao Peng, Jianfeng Pei, and Jiaju Zhou*

Laboratory of Computer Chemistry (LCC), Institute of Process Engineering, Chinese Academy of Sciences, P.O. Box 353, Beijing 100080, People's Republic of China

Received September 16, 2002

A set of epidermal growth factor receptor (EGFR) tyrosine kinase inhibitors was investigated with the aim of developing 3D-QSAR models using the Flexible Atom Receptor Model (FLARM) method. Some 3D-QSAR models were built with high correlation coefficients, and the FLARM method predicted the biological activities of compounds in test set well. The FLARM method also gave the pseudoreceptor model, which indicates the possible interactions between the receptor and the ligand. The possible interactions include two hydrogen bonds, one hydrophobic interaction, and one sulfur−aromatic interaction, which are in accord with those in the pharmacophore model given by the scientists at Novartis. This shows that the FLARM method can bridge 3D-QSAR and receptor modeling in computer-aided drug design. Pharmacophore can be obtained according to these results, and 3D searching can then be done with databases to find the lead compound of EGFR tyrosine kinase inhibitors.

## INTRODUCTION

Protein kinases play an important role in signal transduction pathways regulating a number of cellular functions, such as cell growth, differentiation, and cell death. A variety of tumor types have dysfunctional growth factor receptor tyrosine kinases, resulting in inappropriate mitogenic signaling.[1] Protein tyrosine kinases (PTKs) are, therefore, attractive targets in the search for therapeutic agents not only against cancer but also against many other diseases.[2,3]

About 10 years ago, when research in the signal transduction field was initiated in many pharmaceutical companies, the epidermal growth factor receptor (EGFR) tyrosine kinase was one of the first tyrosine kinases described in the literature, and, therefore, was chosen as a target to start drug discovery projects. Meanwhile, many other receptor and nonreceptor tyrosine kinases have been described and found to be attractive targets for research programs in cancer and noncancer indications.

In the past decades, hundreds, or even thousands of tyrosine kianse inhibitors have been described and reviewed in the literature.[4−26] Within the great number of different structural classes of tyrosine kinase inhibitors, compounds competing with ATP for binding at the catalytic domain of the kinase are considered to be of special interest. Despite the fact that catalytic domains of most protein kinases share significant amino acid sequence homology and conserved core structures, it is now accepted that the ATP-binding site of protein kinases is an exciting target for drug design. Numerous compounds of structurally diverse classes have proved to be highly potent and selective ATP competitive tyrosine kinase inhibitors. Although more than 30 crystal structures of protein kinases complexed with ATP or an ATP competitive inhibitors have been published in the past few years, many attempts to obtain a crystal structure of the EGFR PTK have not been successful.

Recently, several pseudoreceptor modeling methods, alternative 3D-QSAR methods, have been developed and employed in drug design. The receptor modeling method proposed by Walters consists of pseudoatoms at the topological level.[27] Our previous work[28,29] on pseudoreceptors was based on an improvement of Walters' approach. This led to a pseudoreceptor modeling method now implemented in our Flexible Atom Receptor Model (FLARM) software.[30]

FLARM is a new method to do 3D QSAR and receptor modeling. Its basis is GERM and PARM. Our research group developed the method PARM in about 1998 and it can predict bioactivity.[28] And FLARM is an improvement of PARM. Its purpose is to perform 3D QSAR and receptor modeling under the condition that the 3D structure of the target receptor is unavailable. This approach can predict the activity of new drugs. And the explicit atom models can help to understand the mechanism of the interaction between ligands and receptors and even to preliminarily predict the active sites of the real receptors. The open receptor model can provide a better simulation of the real receptor and may rationally correspond to the pharmacophore model. And 3D database searching can then be done with some 3D databases such as NCI-3D or ACD-3D to find new lead compounds. To validate this new approach, some data sets, besides the EGFR tyrosine kinase inhibitors discussed in this paper, were investigated. The first data set was the binding affinity to corticosteroid binding globulin of 21 steroids, probably the most classical system in 3D-QSAR. The $q^2$ was 0.78 for the predicting sets of this system and some pseudoreceptor models were also given. The second data set investigated was the anti-HIV-1 activities of 38 1,1,3-trioxo-2H,4H-thieno[3,4-e][1,2,4]thiadiazine derivatives. The $q^2$ was 0.72 for the predicting sets of this system. And the possible interactions in the pseudoreceptor model were consistent with the results by some other scientists.[30]

In the present paper, the 3D-QSAR of a set of EGFR tyrosine kinase inhibitors was conducted by using the

10.1021/ci0256034 CCC: $25.00 
Published on Web 12/31/2002

**Table 1.** Compounds and Their Biological and Conformational Properties

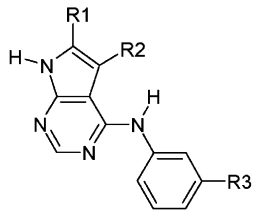


1~4,7~14

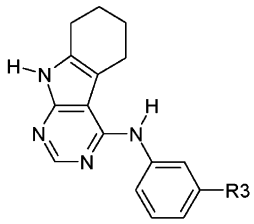


5,28

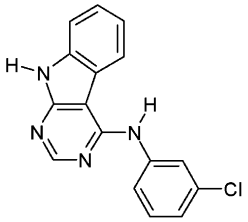


6

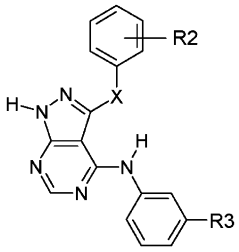


15~22,29~31

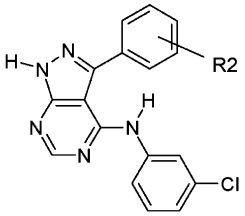


23~27,33

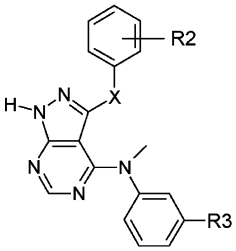


32

| no. | $R_1$ | $R_2$ | $R_3$ | X | $-\log IC_{50}$ (exp.) | no. of conformation[a] | $\Delta E^b$ (kcal/mol) |
|---|---|---|---|---|---|---|---|
| 1 | $CH_3$ | $CH_3$ | Cl | | 7.57 | 8 | 0.21 |
| 2 | $C_6H_5$ | $CH_3$ | Cl | | 7.82 | 13 | 0.45 |
| 3 | $CH_3$ | $C_6H_5$ | Cl | | 6.64 | 6 | 3.36 |
| 4 | $C_6H_5$ | $C_6H_5$ | Cl | | 7.02 | 11 | 3.27 |
| 5 | | | Cl | | 7.54 | 12 | 0.69 |
| 6 | | | | | 8.22 | 8 | 1.04 |
| 7 | $CONHCH_3$ | H | Cl | | 8.52 | 23 | 0.80 |
| 8 | $C_5NH_4$ | H | Cl | | 8.15 | 12 | 0.69 |
| 9 | $C_6H_5OCH_3$ | H | Cl | | 7.82 | 46 | 0.91 |
| 10 | $C_6H_5OH$ | H | Cl | | 8.52 | 12 | 0.80 |
| 11 | $C_6H_5NH_2$(p) | H | Cl | | 8.52 | 11 | 0.80 |
| 12 | $C_6H_5NH_2$(m) | H | Cl | | 8.40 | 24 | 0.82 |
| 13 | $C_6H_5COOH$ | H | Cl | | 9.00 | 67 | 2.73 |
| 14 | $CH_3$ | $CH_3$ | Br | | 7.60 | 9 | 0.23 |
| 15 | | m−Cl | Cl | NH | 7.48 | 68 | 3.48 |
| 16 | | m−OH | Cl | NH | 9.00 | 67 | 3.99 |
| 17 | | $m-OCH_3$ | Cl | NH | 8.10 | 163 | 3.64 |
| 18 | | $p-NH_2$ | Cl | NH | 8.30 | 40 | 3.48 |
| 19 | | H | Cl | $NHCH_2$ | 8.15 | 70 | 3.80 |
| 20 | | m−Cl | Cl | $NHCH_2$ | 7.59 | 136 | 4.54 |
| 21 | | $m-OCH_3$ | Cl | $NHCH_2$ | 8.10 | 214 | 5.93 |
| 22 | | $m-NH_2$ | Cl | $NHCH_2$ | 8.52 | 188 | 5.40 |
| 23 | | p−OH | | | 8.22 | 9 | 1.77 |
| 24 | | H | | | 7.72 | 10 | 2.73 |
| 25 | | $p-OCH_3$ | | | 7.02 | 41 | 2.85 |
| 26 | | m−OH | | | 7.59 | 20 | 2.78 |
| 27 | | $m-NH_2$ | | | 8.30 | 28 | 2.07 |
| 28 | | | Br | | 7.34 | 12 | 0.96 |
| 29 | | m−Cl | Br | NH | 6.89 | 64 | 3.69 |
| 30 | | p−OH | Cl | NH | 8.10 | 36 | 3.52 |
| 31 | | $p-N(CH_3)_2$ | Cl | NH | 7.54 | 76 | 3.92 |
| 32 | | $p-OCH_3$ | Cl | NH | 8.15 | 165 | 5.84 |
| 33 | | $p-NH_2$ | | | 8.70 | 28 | 3.96 |

[a] Number of conformers generated by the random search procedure. [b] Energy difference between the selected and the minimum energy conformer.

FLARM method. In addition to obtaining some 3D-QSAR models, we are more interested to know the possible interactions between the receptor and the ligand. These possible interactions can be seen from the pseudoreceptor model given by the FLARM method. Some compounds with high biological activity can be synthesized and tested basing upon these possible interactions.

## MATERIALS AND METHODS

The 33 compounds considered for this study and their activity expressed as $pKIC_{50}$ are listed in Table 1.[10,11]

**Molecular Modeling.** Molecular modeling was performed by means of the SYBYL software,[31] running on a SGI Octane-2 workstation. Three-dimensional models of all

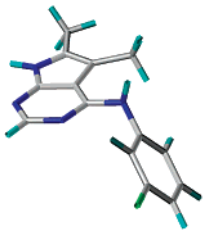

**Figure 1.** The selected conformation of compound **1**, the template molecule. The energy of this conformation is higher than the minimum energy conformer by only 0.21 kcal/mol.

molecules were built by assembling fragments from the SYBYL standard library.

The conformational space of each molecule was sampled by means of the RANDOMSEARCH procedure of SYBYL. In this Monte Carlo-like method, a number of conformations are generated by randomly rotating selected bonds of the molecules. The degree of completeness of the analysis can be regulated by setting a number of parameters: energy cutoff, number of times one conformer is found, and number of attempts to find a new conformer. In practice, the energy cutoff was set about 50 kcal/mol above the estimated total energy of the molecule, the maximum number of hits was 6, and the maximum number of attempts was 1000. The conformations generated by RANDOMSEARCH were subsequently submitted to the selection of conformations. MOPAC charges were calculated with the aid of the semiempirical, quantum-chemical procedure AM1 within the SYBYL program package.

**FLARM Computation.** With regard to the alignment, compound **1** was selected as the template molecule, and each conformation of all remaining compounds was examined in order to find the one providing the best overlap of the pyrrolo[2,3-d]pyrimidine or the pyrazolo[3,4-d]pyrimidine ring. The crystal structure of compound **1** was not found in the Cambridge Structural Database (CSD). According to ref 9, the conformation shown in Figure 1 was selected as the aligned conformation, whose energy is higher than the minimum energy conformer by only 0.21 kcal/mol (Figure 1). The FLARM computation was conducted with the alignment result of all compounds. The cushion between the receptor and the ligand was 0.5 Å. The atom number of the receptor was 45. The genetic population size was 120, and the genetic evolvement was completed when the cross-validated correlation coefficient reached 0.88. The computation took about 9 min on a Pentium II 350 MHz PC.

## RESULTS

**3D-QSAR Models.** A series of 3D-QSAR models were obtained by using the FLARM method. The top 15 models are presented in Table 2. Model 2 was taken as the final model because its test set performance was the best. In this model, the cross-validated correlation coefficient was 0.915, and the standard deviation of the fit was 0.173. In every model in Table 2, the difference between $q^2$ and $r^2$ is very small, less than 0.026.

**Testing of 3D-QSAR Models.** To test the stability and predictive ability of the 3D-QSAR models built with FLARM method, six compounds (**28**−**33**), which were not included in the construction of FLARM models, were selected as a test set for validation. The results are simultaneously shown in Table 3 and Figure 2, and the predicted $-\log IC_{50}$ values are in good agreement with the experimental data in a statistically tolerable error range.

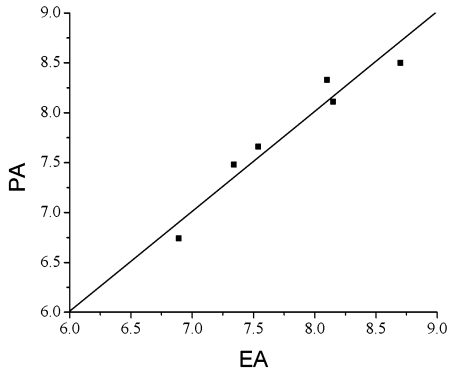


**Figure 2.** Correlation between the predicted activities (PA) by FLARM and the experimental inhibitory potencies ($-\log IC_{50}$). The correlation coefficient and the standard deviation are 0.965 and 0.191, respectively.

**Table 2.** Top 15 Models Given by FLARM[a]

| model | $a$ | $b$ | $r^2$ | $q^2$ | SD |
|---|---|---|---|---|---|
| 1 | 6.51861 | −0.446510 | 0.920783 | 0.920926 | 0.165538 |
| 2 | 6.34787 | −0.471984 | 0.913472 | 0.915476 | 0.173009 |
| 3 | 6.45497 | −0.461943 | 0.915827 | 0.913042 | 0.170638 |
| 4 | 6.69127 | −0.424812 | 0.911742 | 0.909436 | 0.174730 |
| 5 | 6.87368 | −0.463002 | 0.903925 | 0.883523 | 0.182304 |
| 6 | 5.97042 | −0.555084 | 0.901007 | 0.883318 | 0.185051 |
| 7 | 6.74575 | −0.436194 | 0.900619 | 0.879658 | 0.185414 |
| 8 | 6.77198 | −0.458973 | 0.900544 | 0.878366 | 0.185484 |
| 9 | 6.48777 | −0.420381 | 0.894594 | 0.871025 | 0.190951 |
| 10 | 6.61797 | −0.354150 | 0.890711 | 0.867806 | 0.194437 |
| 11 | 7.46703 | −0.514965 | 0.890765 | 0.867795 | 0.194388 |
| 12 | 6.49585 | −0.498512 | 0.889259 | 0.867459 | 0.195724 |
| 13 | 6.62269 | −0.469899 | 0.884408 | 0.858995 | 0.199964 |
| 14 | 6.26017 | −0.516120 | 0.875825 | 0.854013 | 0.207255 |
| 15 | 6.75121 | −0.423081 | 0.873873 | 0.850712 | 0.208878 |

[a] The meaning of $a$ and $b$ is that activity ($-\log IC_{50}$) = $a + b \times$ energy (kcal/mol) and SD is the standard deviation of cross-validated fitting.

**Table 3.** Prediction Results by FLARM Method

| no. | $-\log IC_{50}$ (exp.) | $-\log IC_{50}$ (FLARM) | residual |
|---|---|---|---|
| 28 | 7.34 | 7.48 | −0.14 |
| 29 | 6.89 | 6.74 | 0.15 |
| 30 | 8.10 | 8.33 | −0.23 |
| 31 | 7.54 | 7.66 | −0.12 |
| 32 | 8.15 | 8.11 | 0.04 |
| 33 | 8.70 | 8.50 | 0.20 |

**The Novartis Pharmacophore Model.** Furet et al. published the first data of a pharmacophore model for inhibitors competing for the ATP-binding site of the EGFR PTK.[32] In the course of this work, a hypothetical model for the binding mode of the protein kinase inhibitor staurosporine in the ATP-binding site of the cAMP-dependent protein kinase was developed by using the published crystal data of this kinase. Recently, a published crystal structure of a complex of staurosporine with cyclin-dependent kinase (CDK2) fully confirmed the proposed binding mode of staurosporine.[33] In addition, the binding hypothesis was fully consistent with a model of the EGFR PTK constructed by homology to the X-ray crystal structure of the cAMP-dependent protein kinase. This pharmacophore model has then been used successfully for the design and synthesis of

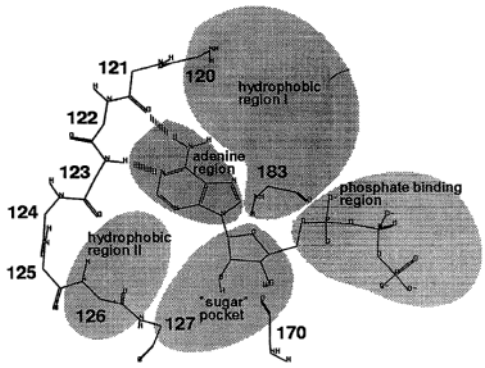


**Figure 3.** Protein tyrosine kinase pharmacophore model given by scientists at Novartis. The kinase is cAMP-dependent protein tyrosine kinase and the ligand is ATP.[9]

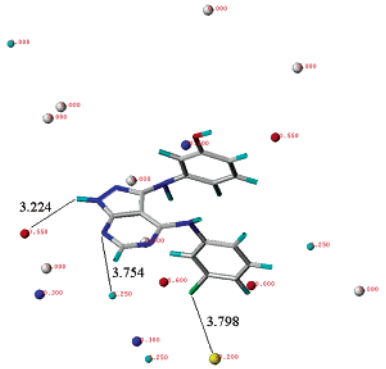


**Figure 4.** Pseudoreceptor model given by FLARM. The ligand is compound **16**, and the numbers indicate the distances between the corresponding atoms (Å).

many compounds.[8−12] Together with the availability of published crystal data of several protein kinases, the model was refined and is now of general usefulness for the design of protein tyrosine kinase inhibitors.[9] According to this pharmacophore model, the ATP-binding site in protein tyrosine kinases can be divided into five regions, shown in Figure 3. In these five regions, hydrophobic region II and phosphate binding region are not of primary importance with respect to binding affinity, though they can be useful to improve the selectivity of inhibitors. The other three regions, namely, adenine region, sugar pocket, and hydrophobic region I, are primaryly important to the binding affinity.

**Pseudoreceptor Model.** The pseudoreceptor model given by FLARM is shown as Figure 4. The ligand in Figure 4 is compound **16**. The numbers in Figure 4 indicate the distances between the corresponding atoms (Å). The atom number of this pseudoreceptor is actually 20, and the other 25 atoms are all void atoms. This is one character of the FLARM method, which makes the method meaningful and effective.

Three interactions between the receptor and the ligand can be easily seen from the pseudoreceptor model in Figure 4.

The first interaction is the hydrogen bond between the NH in the ligand and the oxygen atom in the receptor, and the distance between these two atoms is 3.224 Å. In the Novartis pharmacophore model, this hydrogen bond is between the NH and Gln 767 in the EGFR PTK. The interaction in the pseudoreceptor model is in accord with that in the Novartis pharmacophore model, and the two models both have an oxygen atom at this position (Figures 3 and 4).

The second interaction is also a hydrogen bond between the N1 in the ligand and the hydrogen atom in the receptor,

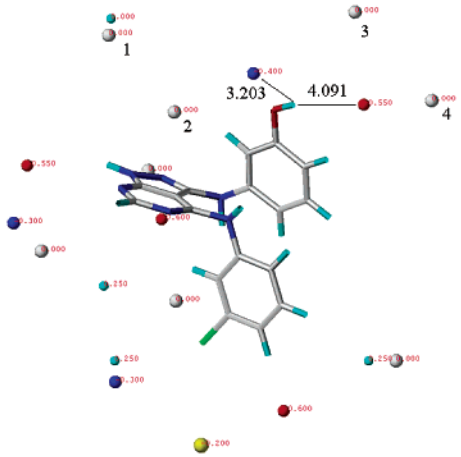


**Figure 5.** Pseudoreceptor model given by FLARM (another view). The ligand is compound **16**, and the numbers indicate the distances between the corresponding atoms (Å).

and the distance between these two atoms is 3.754 Å. In the Novartis pharmacophore model, this hydrogen bond is between the N1 and Met 769 in the EGFR PTK. The interaction in the pseudoreceptor model is in accord with that in the Novartis pharmacophore model, and the two models both have a hydrogen atom at this position (Figures 3 and 4).

The third interaction is a sulfur−aromatic interaction between the chlorophenyl group in the ligand and the sulfur atom in the receptor, and the distance between the chlorine atom and the sulfur atom is 3.798 Å. In the Novartis pharmacophore model, this interaction is between the chlorophenyl group and the Cys 773 of the EGFR PTK. The interaction in the pseudoreceptor model is in accord with that in the Novartis pharmacophore model, and the two models both have a sulfur atom at this position (Figures 3 and 4).

As to the ligand (compound **16**) in Figure 4, two additional hydrogen bonds are assumed in the Novartis pharmacophore model: one between the N6 of the pyrazole ring and the side chain of Thr 766, the other between the hydroxyl group of the phenol moiety and the backbone of Phe 832. The former hydrogen bond is not seen in the pseudoreceptor model, but the latter hydrogen bond can be evidently observed from the pseudoreceptor model, shown in Figure 5. There are two possible hydrogen bond acceptors around the hydroxyl group, one nitrogen atom and the other oxygen atom. The distances are 3.203 and 4.091 Å, respectively.

Another possible interaction between the ligand and the receptor can be seen from Figure 5, namely, hydrophobic interaction. There are four neutral carbon atoms labeled 1, 2, 3, and 4 near the phenol moiety. These four carbon atoms make a parallelogram approximately. This indicates that there is a hydrophobic interaction between the ligand and the receptor. The four carbon atoms are equivalent to the hydrophobic region I in the Novartis pharmacophore model. The hydroxy group makes the phenol moiety less hydrophobic, but a hydrogen bond is formed instead. Compound **16**, therefore, still has high biological activity. Actually, it is one of the most potent compounds ($-\log IC_{50} = 9.00$).

**Comparison of Pseudoreceptor Model and Novartis Pharmacophore Model.** The so-called active sites can be obtained from the possible interactions between the ligand

and the pseudoreceptor model given by FLARM. The results acquired by FLARM are in accord with the Novartis pharmacophore model. The inhibitors investigated in this paper were synthesized and assessed by the scientists at Novartis. And the pharmacophore model was put forward and confirmed by some new active compounds. The agreement with this pharmacophore can prove the validity of this approach in this system. The Novartis pharmacophore model was obtained based on the published crystal data of the cAMP-dependent tyrosine kinase and homology between this kinase and the EGFR tyrosine kinase. And FLARM is a pseudoreceptor model method. These two results, acquired with quite different methods, are in accord with each other. On one hand, this means that these two models can validate each other. On the other hand, this tells us that many different methods can all be used in the course of computer-aided drug design. As to the pseudoreceptor model given by FLARM, it can be used to predict the possible interactions between the receptor and the ligand and then bridges 3D-QSAR and receptor modeling. In the pseudomodel given by current FLARM, the distances between the atoms in the pseudoreceptor and the ligand are a little further than normal distances, such as the distance of hydrogen bonds, which will be solved in the next version of FLARM.

The validity of FLARM resulted from its following characteristics: (1) Flexible receptor model—FLARM introduced the concept of flexible receptor model in order to avoid the bias of the arbitrary receptor shape that is sensitive to the training set. All the atoms in a FLARM receptor model are spatially moveable in the process of genetic evolving. (2) Open receptor model—Usually, ligands were fully closed in a receptor model generated by the previous methods. But in the real world, there were cases that ligands were only partly enwrapped in receptors. FLARM can produce open receptor models that allow large gaps. An open model may provide a better simulation of the real receptor and may rationally correspond to the pharmacophore model. Moreover, a closed model containing redundant noise information may hurt the predicting ability of the model and may be too tight for the ligands in test set to dock into. (3) Improved Genetic Algorithm (IGA)—The FLARM computation was rather quick. For example, FLARM computation on the system of EGFR tyrosine kinase inhibitors took only about 9 min on a Pentium II 350 MHz PC.

## CONCLUSIONS

A set of EGFR tyrosine kinase inhibitors was investigated with the aim of developing 3D-QSAR models using the FLARM method. Some 3D-QSAR models were built with high correlation coefficients, and the FLARM method predicted the biological activities of compounds in test set well. The FLARM method also gave the pseudoreceptor model, which indicates the possible interactions between the receptor and the ligand. These possible interactions include two hydrogen bonds, one hydrophobic interaction and one sulfur−aromatic interaction, which are in accord with those in the Novartis pharmacophore model. This shows that the FLARM method can bridge 3D-QSAR and receptor modeling in computer-aided drug design.

The active sites given by the FLARM method is in accord with those in the Novartis pharmacophore model. The FLARM method is a pseudoreceptor model method, which belongs to alternative 3D-QSAR methods. And the Novartis pharmacophore model is obtained based on the published crystal data of the cAMP-dependent tyrosine kinase and homology between this kinase and the EGFR tyrosine kinase. The active sites result is in accord with each other though the method and the approach are quite different. So many different methods can all be used in the course of computer-aided drug design.

Pharmacophore can be obtained according to the Novartis pharmacophore model and the pseudoreceptor model given by the FLARM method. 3D searching can then be done with the NCI-3D or other 3D databases to find the lead compound of tyrosine kinase inhibitors.

## ACKNOWLEDGMENT

The authors are grateful for the financial support from the State Key Program of Basic Research of China (Grant 1998051115).

## REFERENCES AND NOTES

(1) Aaronson, S. A. Growth factors and cancer. *Science* **1991**, *254*, 1146−1152.
(2) Fry, D. W.; Kraker, A. J.; Conners, R. C.; Elliott, W. L.; Nelson, J. M.; Showalter, H. D.; Leopold, W. R. Strategies for the discovery of novel tyrosine kinase inhibitors with anticancer activity. *Anti-Cancer Drug Des*. **1994**, *9*, 331−351.
(3) Levitzki, A.; Gazit, A. Tyrosine kinase inhibition: An approach to drug development. *Science* **1995**, *267*, 1782−1788.
(4) Fry, D. W. Protein tyrosine kinases as therapeutic targets in cancer chemotherapy and recent advances in the development of new inhibitors. *Exp. Opin. Invest. Drugs* **1994**, *3*, 577−595.
(5) Traxler, P.; Lydon, N. Recent advances in protein tyrosine kinase inhibitors. *Drugs Future* **1995**, *20*, 1261−1274.
(6) Spada, A. P.; Myers, M. R. Small molecule inhibitors of tyrosine kinase activity. *Exp. Opin. Ther. Patents* **1995**, *5*, 805−817.
(7) Bridges, A. J. The current status of tyrosine kinase inhibitors: do the diarylamine inhibitors of the EGF receptor represent a new beginning? *Exp. Opin. Ther. Patents* **1995**, *5*, 1245−1257.
(8) Traxler, P. Protein tyrosine kinase inhibitors in cancer treatment. *Exp. Opin. Ther. Patents* **1997**, *7*, 571−588.
(9) Traxler, P.; Furet, P. Strategies toward the design of novel and selective protein tyrosine kinase inhibitors. *Pharmacol. Ther.* **1999**, *82*, 195−206.
(10) Traxler, P.; Furet, P.; Mett, H.; Buchdunger, E.; Meyer, T.; Lydon, N. 4-(Phenylamino)pyrrolopyrimidines: potent and selective, ATP site directed inhibitors of the EGF-receptor protein tyrosine kinase. *J. Med. Chem.* **1996**, *38*, 2285−2292.
(11) Traxler, P.; Bold, G.; Frei, J.; Lang, M.; Lydon, N.; Mett, H.; Buchdunger, E.; Meyer, T.; Mueller, M.; Furet, P. Use of a pharmacophore model for the design of EGF-R tyrosine kinase inhibitors: 4-(phenylamino)pyrazolo-pyrimidines. *J. Med. Chem.* **1997**, *40*, 3601−3616.
(12) Traxler, P.; Green, J.; Mett, H.; Sequin, U.; Furet, P. Use of a pharmacophore model for the design of EGFR tyrosine kinase inhibitors: isoflavones and 3-phenyl-4(1*H*)-quinolones *J. Med. Chem.* **1999**, *42*, 1018−1026.
(13) Rewcastle, G. W.; Denny, W. A.; Bridges, A. J.; Zhou, H.; Cody, D. R.; McMichael, A.; Fry, D. W. Tyrosine kinase inhibitors. 5. Synthesis and structure−activity relationships for 4-(phenylmethyl-amino)-and 4-(phenylamino) quinazolines as potent adenosine 5′-triphosphate binding site inhibitors of the tyrosine kinase domain of the epidermal growth factor receptor. *J. Med. Chem.* **1995**, *38*, 3482−3487.
(14) Showalter, H.; Sercel, A.; Leja, B. Tyrosine kinase inhibitors. 6. Structure- activity relationships among *N*- and 3-substituted 2,2′-diselenobis (1*H*-indoles) for inhibition of protein tyrosine kinases and comparative in vitro and in vivo studies against selected sulfur congeners. *J. Med. Chem.* **1997**, *40*, 413−426.
(15) Thompson, A. M.; Bridges, A. J.; Fry, D. W.; Kraker, A. J.; Denny, W. A. Tyrosine kinase inhibitors. 7. 7-amino-4-(phenylamino)- and 7-amino-4-[(phenyl-methyl)amino-lpyrido[4,3-d] pyrimidines: A new class of inhibitors of the tyrosine kinase activity of the epidermal growth factor receptor. *J. Med. Chem.* **1995**, *38*, 3780−3788.
(16) Bridges, A.; Zhou, H.; Cody, D. Tyrosine kinase inhibitors. 8. An unusually steep structure−activity relationship for analogues of 4-(3-

bromoanilino)-6, 7-dimethoxyquinazoline (PD 153035), a potent inhibitor of the epidermal growth factor receptor. *J. Med. Chem.* **1996**, *39*, 267−276.

(17) Rewcastle, G. W.; Palmer, B. D.; Bridges, A. J.; Showalter, H. D.; Sun, L.; Nelson, J. M.; McMichael, A.; Kraker, A. J.; Fry, D. W.; Denny, W. A. Tyrosine kinase inhibitors. 9. Synthesis and evaluation of fused tricyclic quinazolines analogues as ATP site inhibitors of the tyrosine kinase activity of the epidermal growth factor receptor. *J. Med. Chem.* **1996**, *39*, 918−928.

(18) Rewcastle, G. W.; Palmer, B. D.; Thompson, A. M.; Bridges, A. J.; Cody, D. R.; Zhou, H.; Fry, D. W.; McMichael, A.; Kraker, A. J.; Denny, W. A. Tyrosine kinase inhibitors. 10. Isomeric 4-[(3-bromophenyl)-amino]pyrido[d]-pyrimidines are potent ATP binding site inhibitors of the tyrosine kinase function of the epidermal growth factor receptor. *J. Med. Chem.* **1996**, *39*, 1823−1835.

(19) Palmer, B.; Trumpp-Kallmeyer, S.; Fry, D. Tyrosine kinase inhibitors. 11. soluble analogues of pyrrolo- and pyrazoloquinazolines as epidermal growth factor receptor inhibitors: synthesis, biological evaluation, and modeling of the mode of binding. *J. Med. Chem.* **1997**, *40*, 1519−1529.

(20) Rewcastle, G.; Bridges, A.; Fry, D. Tyrosine kinase inhibitors. 12. synthesis and structure−activity relationships for 6-substituted 4-(phenylamino)pyrimido[5, 4-*d*]pyrimidines designed as inhibitors of the epidermal growth factor receptor. *J. Med. Chem.* **1997**, *40*, 1820−1826.

(21) Thompson, A.; Murray, D.; Elliott, W. Tyrosine kinase inhibitors. 13. structure-activity relationships for soluble 7-substituted 4-[(3-bromophenyl)amino]pyrido[4,3-*d*]pyrimidines designed as inhibitors of the tyrosine kinase activity of the epidermal growth factor receptor. *J. Med. Chem.* **1997**, *40*, 3915−3925.

(22) Rewcastle, G.; Murray, D.; Elliott, W. Tyrosine kinase inhibitors. 14. structure -activity relationships for methyl-amino-substituted derivatives of 4-[(3-bromo-phenyl)amino]-6-(methylamino)-pyrido[3,4-*d*]-pyrimidine (PD 158780), a potent and specific inhibitor of the tyrosine kinase activity of receptors for the EGF family of growth factors. *J. Med. Chem.* **1998**, *41*, 742−751.

(23) Smaill, J.; Palmer, B.; Rewcastle, G. Tyrosine kinase inhibitors. 15. 4-(phenylamino)quinazoline and 4-(phenylamino)pyrido[*d*]pyrimidine acrylamides as irreversible inhibitors of the ATP binding site of the epidermal growth factor receptor. *J. Med. Chem.* **1999**, *42*, 1803−1815.

(24) Showalter, H.; Gridges, A.; Zhou, H. Tyrosine kinase inhibitors. 16. 6,5,6-tricyclic bnzothieno[3, 2-*d*]pyrimidines and primido[5, 4-*b*]- and -[4,5-*b*]indoles as potent inhibitors of the epidermal growth factor receptor Tyrosine Kinase. *J. Med. Chem.* **1999**, *42*, 5464−5474.

(25) Smaill, J.; Showatle, H. Tyrosine kinase inhibitors. 17. Irreversible inhibitors of the epidermal growth factor receptor: 4-(phenylamino)-quinazoline- and 4-(phenylamino)pyrido[3,2-*d*]pyrimidine-6-acrylamides bearing additional solubilizing functions. *J. Med. Chem.* **2000**, *43*, 1380−1397.

(26) Smaill, J.; Showalte, H.; Zhou, H. Tyrosine kinase inhibitors. 18. 6-substituted 4-anilinoquinazolines and 4-anilinopyrido[3,4-*d*]pyrimidines as soluble, irreversible inhibitors of the epidermal growth factor receptor. *J. Med. Chem.* **2001**, *44*, 429−440.

(27) Walters, D. E.; Hinds, R. M. Genetically evolved receptor models: A computational approach to construction of receptor models. *J. Med. Chem.* **1994**, *37*, 2527−2536.

(28) Chen, H.; Zhou, J.; Xei, G. PARM: A genetic evolved algorithm to predict bioactivity. *J. Chem. Inf. Comput. Sci.* **1998**, *38*, 243−250.

(29) Pei, J.; Zhou, J.; Xie, G.; Chen, H.; He, X. PARM: A practical utility for drug design. *J. Mol. Graph. Model.* **2001**, *19*, 448−454.

(30) Pei, J.; Zhou, J. Flexible atom receptor model (FLARM). *Acta Chim. Sinica* **2002**, *60*, 973−979.

(31) *Sybyl*, version 6.5; Tripos Associates: St. Louis, MO, 1998.

(32) Furet, P.; Caravatti, G.; Lydon, N.; Priestle, J.; Sowadski, J.; Trinks, U.; Traxler, P. Modeling study of protein kinase inhibitors: binding mode of staurosporine − origin of the selectivity of CGP 52411. *J. Comput. Aided Mol. Des.* **1995**, *9*, 465−471.

(33) Lawie, A. M.; Noble, M. E. M.; Tunnah, P.; Brown, N. R.; Johnson, L. N. Endicott, J. A. Protein kinase inhibition by staurosporine revealed in details of the molecular interaction with CDK2. *Nature Struct. Biol.* **1997**, *4*, 796−801.

CI0256034